Calculated details of a mechanism for conversion of N_2 to NH_3 at the FeMo cluster of nitrogenase

Ian Dance

School of Chemistry, University of New South Wales, Sydney 2052, Australia

Density functional calculations mapping the geometry/energy hypersurface of the Fe_7MoS_9(*S*-cysteine)-(homocitrate)(histidine) cluster in nitrogenase and its binding of N_2, H^+, e^- and N–H intermediates reveal mechanistic details for the formation of NH_3.

The enzyme nitrogenase reduces N_2 to NH_3 at an Fe_7MoS_9(*S*-cysteine)(homocitrate)(histidine) cluster. While the structure of this active site is known in atomic detail, the mechanism for binding, activation, electronation and protonation of N_2 is still tantalisingly obscure.[1] In addition to numerous reports of model systems, and commentaries on chemical expectations about mechanism,[2] there are theoretical contributions to investigation of the mechanism which include calculations of N_2 binding geometries and electronic structure,[3] and a mechanism supported by density functional calculations has been outlined.[4]

Here I communicate new density functional calculations† mapping the geometry/energy hypersurface of the full cluster, as it binds the reactants N_2, H^+ (and e^-), rearranges the intermediate N–H species, and facilitates the sequential release of $2NH_3$.

Fig. 1 defines the 40 atoms included in the model of the active site. The redox level adopted as the reference state in the following corresponds to a core $[Fe_7Mo]^{22+}$, equivalent to $(Fe^{+2.57})_7Mo^{4+}$. As previously described[4] the protein surrounds favour one undercoordinated $(Fe^3)_4(S^3)_2(S^2)_2$ face‡ (Fe^{3A}, Fe^{3B}, Fe^{3C}, Fe^{3D} in Fig. 1) as the reactive site. Fig. 2 shows three configurations for N_2 bound to this site: the lowest energy configuration has the least symmetrical geometry, and is dubbed the oblique arrow configuration. This optimised binding geometry differentiates the proximal N atom (N^p) bound to four Fe atoms, and the distal N atom (N^d) bound to two Fe atoms.

A characteristic of the oblique arrow configuration is that the distal N atom (N^d) is positioned between three of the

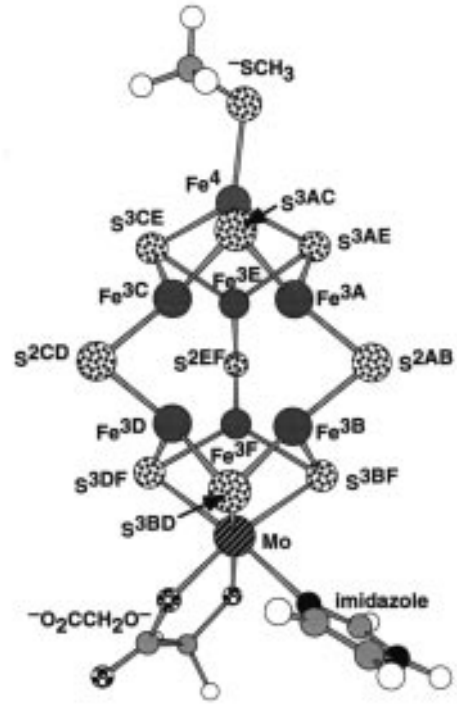

Fig. 1 The $[Fe_7MoS_9(SCH_3)(imidazole)(O_2CCH_2O)]$ model calculated as the active site of nitrogenase. Numerical superscripts in atom identifiers are coordination numbers: N, black; C, small grey; H, open.

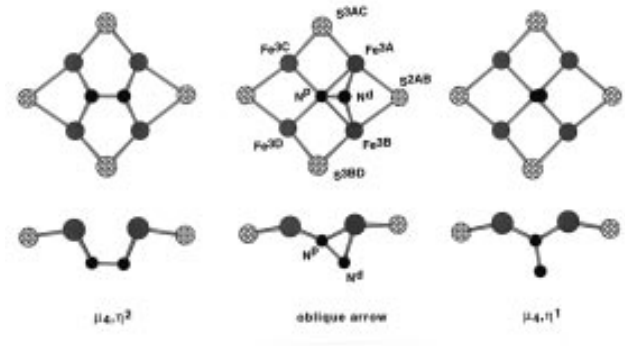

Fig 2 The μ_4,η^2, oblique arrow and μ_4,η^1 geometries for N_2 bound to the Fe^{3A} Fe^{3B} Fe^{3C} Fe^{3D} face, with relative energies +83, 0, +37 kJ mol^{-1}. Other atoms (Fig. 1) included in the energy minimisations are omitted for clarity. In the lowest energy geometry, N^p, N^d are proximal and distal to the Fe_4 face respectively: N^p–Fe^3 1.93–1.98 Å; N^d–Fe^{3A},Fe^{3B} 2.07, 2.03 Å; Fe^{3A}–Fe^{3C} 2.66, Fe^{3B}–Fe^{3D} 2.64 Å, Fe^{3A}–Fe^{3B} 2.65 Å, Fe^{3C}–Fe^{3D} 2.56 Å.

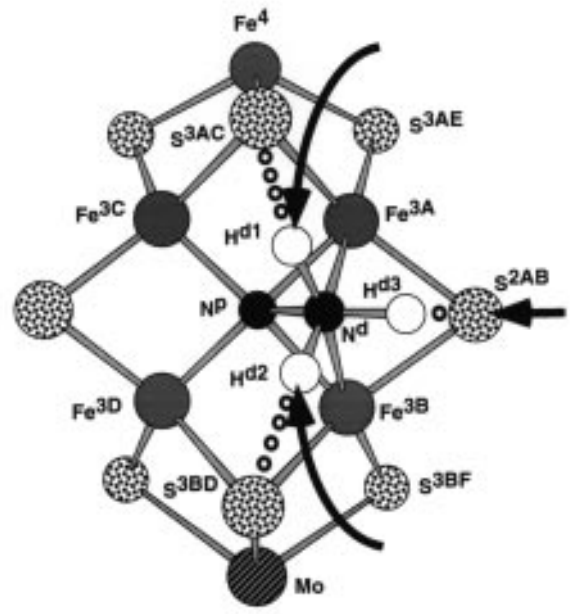

Fig 3 Location of hydrogen atoms (H^{d1}, H^{d2}, H^{d3}) on N^d prior to dissociation of N^dH_3. The rear Fe^3 and S^2 atoms and the complete coordination of Fe^4 and Mo are not shown for reasons of clarity. Open heavy circles show the hydrogen bonds from H to S^3 and S^2. Heavy arrows show probable trajectories for the three approaching hydrogen atoms (see text).

surrounding S atoms, S^{2AB}, S^{3AC}, S^{3BD}, such that protons on these S atoms are well positioned for transfer to N^d. Further, addition of two electrons to the cluster at this stage most affects the electron population at these S atoms: the changes in Mulliken partial charges are *ca.* −0.19 at S^2, *ca.* −0.11 at S^3, −0.04 at Mo, and *ca.* 0.00 at Fe. Therefore the possibility of reduction and protonation of the distal N atom was investigated by energy minimisation of a structure containing three H atoms between N^d and S, hydrogen bonded to S, as detailed in Fig. 3. The electronic population at this stage was equivalent to addition of N_2, $4e^-$ and $3H^+$ relative to the reference state. Energy minimisation caused scission of the N–N bond and dissociation of the distal N atom as NH_3: Fig. 4 shows several stages in this dissociation. Because the calculation did not include the surrounding protein and its hydrogen bond acceptor sites, the dissociating NH_3 retains its hydrogen bonds to the three S atoms, and inverts during the dissociation; Fig. 4(*d*) also shows a later stage of dissociation after the hydrogen bonds have been broken.

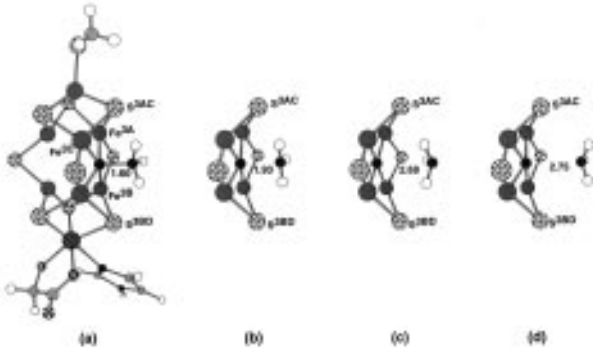

Fig 4 Side views of four stages in the dissociation of N^dH_3, shown fully for stage (*a*) and as the dissociation face only for (*b*)–(*d*). $N^p\cdots N^l$ distances (Å) are marked (the N–N bond length at the beginning of this reaction was 1.28 Å). Relative energies for these intermediates are (*a*) 0, (*b*) −188, (*c*) –368, (*d*) –414 kJ mol^{-1}. Stages (*b*) and (*c*) demonstrate the inversion of NH_3 due to the strength of the S···H hydrogen bonds, which are broken in stage (*d*).

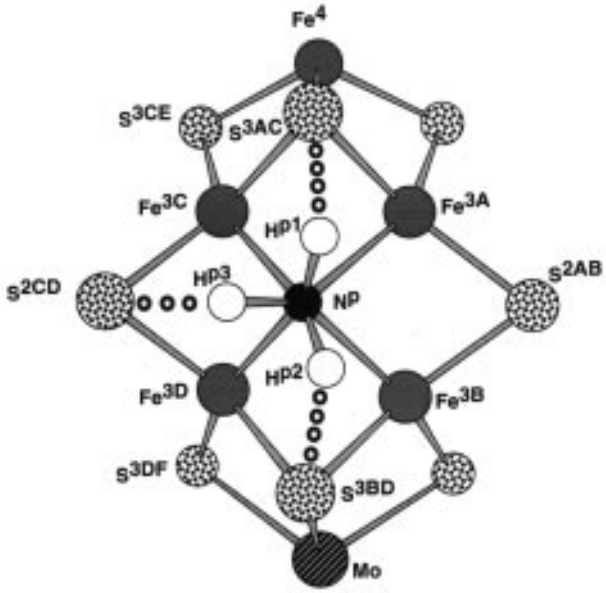

Fig. 5 Location of hydrogen atoms (H^{p1}, H^{p2}, H^{p3}) on N^p prior to dissociation of N^pH_3. The rear Fe^3 and S^2 atoms and the complete coordination of Fe^4 and Mo are not shown for reasons of clarity. Open heavy circles show the hydrogen bonds from H to S^3 and S^2.

After dissociation of N^dH_3 the proximal N atom is left bound to the Fe_4 face; the second stage of electronation and protonation of this N atom can also involve the surrounding S atoms, but the geometry is different because N^p is close to the Fe_4 face. Fig. 5 shows an intermediate geometry containing three new H atoms associated with N^p and hydrogen bonded to S^2 and S^3. On energy minimisation with an atom/electron population now corresponding to the reference state + N_2 + $6e^-$ + $6H^+$ − NH_3, N^dH_3 dissociates by sliding around one of the Fe^3 atoms.

These results provide the rudiments of a mechanism for binding of N_2, proton approach, introduction of electrons, and sequential dissociation of NH_3. They reinforce the chemical expectation that undercoordinated Fe^3 and S^2 atoms play key roles. During the processes described the Fe–Fe, Fe–S and S–Mo distances change as expected according to increases and decreases in coordination. Additional calculations reveal that H atoms can also bridge Fe^3–S^3 bonds, and that Fe^3 atoms as well as the Fe^3–S^3 bonds can mediate the passage of H atoms from protein to both the distal and proximal N atoms: likely trajectories for H approach to N^d are shown in Fig. 3. Other mechanistic aspects currently being refined involve protonation and/or electronation of N_2 *en route* to the oblique arrow configuration, protonation/electronation of N^p while N^dH_3 is dissociating, and the coupled formation of H_2. Further development will include relevant surrounding protein, which is essential for the ingress of protons and the egress of NH_3.

The support of this research by the Australian Research Council is gratefully acknowledged.

Footnotes

† Calculations used non-local blyp functionals and double numerical basis sets, as implemented in the program DMol (MSI). The accuracy of these methods has been demonstrated by replication of the experimental geometries of related clusters such as $VFe_4S_6(SR)(PR_3)_4$.[5] All models have C_1 symmetry.

‡ Numerical superscripts signify coordination numbers.

References

1 M. K. Chan, J. Kim and D. C. Rees, *Science*, 1993, **260**, 792; J. T. Bolin, A. E. Ronco, T. V. Morgan, L. E. Mortenson and N. H. Xuong, *Proc. Natl. Acad. Sci. USA*, 1993, **90**, 1078; D. C. Rees, M. K. Chan and J. Kim, *Adv. Inorg. Chem.*, 1993, **40**, 89; J. Kim and D. C. Rees, *Biochemistry*, 1994, **33**, 389; J. B. Howard and D. C. Rees, *Annu. Rev. Biochem.*, 1994, **63**, 235.

2 R. R. Eady and G. J. Leigh, *J. Chem. Soc., Dalton Trans.*, 1994, 2739; G. J. Leigh, *New J. Chem.*, 1994, **18**, 157; *Science*, 1995, **268**, 827; T. A. Bazhenova and A. E. Shilov, *Coord. Chem. Rev.*, 1995, **144**, 69; C. E. Laplaza and C. C. Cummins, *Science*, 1995, **268**, 861; C. E. Laplaza, A. R. Johnson and C. C. Cummins, *J. Am. Chem. Soc.*, 1996, **118**, 709; R. L. Richards, *Pure Appl. Chem.*, 1996, **68**, 1521; D. Coucouvanis, *J. Biol. Inorg. Chem.*, 1996, in the press; C. J. Pickett, *J. Biol. Inorg. Chem.*, 1996, in the press; D. Sellmann and J. Sutter, *J. Biol. Inorg. Chem.*, 1996, in the press; R. N. F. Thorneley and D. J. Lowe, *J. Biol. Inorg. Chem.*, 1996, in the press.

3 H. Deng and R. Hoffmann, *Angew. Chem., Int. Ed. Engl.*, 1993, **32**, 1062; W. Plass, *J. Mol. Struct.*, 1994, **315**, 53; R. J. Deeth and C. N. Field, *J. Chem. Soc., Dalton Trans.*, 1994, 1943; R. J. Deeth and S. A. Langford, *J. Chem. Soc., Dalton Trans.*, 1995, 1; K. K. Stavrev and M. C. Zerner, *Chem. Eur. J.*, 1996, **2**, 83; Q. Cui, D. G. Musaev, M. Svensson, S. Sieber and K. Morokuma, *J. Am. Chem. Soc.*, 1995, **117**, 12366.

4 I. G. Dance, *Aust. J. Chem.*, 1994, **47**, 979.

5 I. G. Dance, *ACS Symp. Ser.*, ed. E. I. Steifel and K. Matsumoto, American Chemical Society, Washington DC, 1996, in the press.

Received, 21st October 1996; Com. 6/07136H